Attractor splitting induced by resonant perturbations

V. N. Chizhevsky,* R. Corbalán,† and A. N. Pisarchik*
Departament de Física, Universitat Autònoma, de Barcelona, E-08193, Bellaterra (Barcelona), Spain
(Received 3 March 1997)

We present experimental and numerical results which demonstrate that the so-called nonfeedback control of chaos fundamentally changes the nature of nonautonomous systems. We show that additional weak resonant perturbations (i) induce bistability, splitting the primary attractor into two new ones, and (ii) shift all bifurcation points for these two coexisting attractors in opposite directions as the perturbation amplitude changes. Both perturbation-induced bistability and shift strongly depend on the phase difference between the perturbation and fundamental frequencies. [S1063-651X(97)08008-2]

PACS number(s): 05.40.+j, 42.55.Lt

The effect of resonant perturbations on the dynamics of nonlinear systems has attracted much attention recently. This is motivated by the fact that weak periodic perturbations at a subharmonic frequency, used in the so-called nonfeedback control technique, can suppress chaos [1]. Recently [2], it has been experimentally demonstrated with a loss-modulated CO_2 laser that resonant perturbations, depending on their phase and amplitude, can suppress not only chaos but any periodic orbit, or induce chaos and a crisis of strange attractors [3]. Up to now the main attention has been paid to the question of how resonant perturbations modify the dynamics of nonlinear systems. This raises another question, namely, whether the system itself is essentially modified by introducing the weak resonant perturbation. By essential modifications we mean the appearance of new attractors in the system induced by weak resonant perturbations. Recently [4], it has been theoretically shown from an analysis of a logistic map that feedback control [5] may induce new attractors in optical systems.

In this paper we show, both experimentally and numerically, that weak parametric perturbations at subharmonic frequency (i) induce bistability in the system, so that instead of one primary (initial) attractor at least two attractors appear in the system (moreover, these new attractors appear just above the first shifted bifurcation point), and (ii) shift all bifurcation points belonging to these new branches in opposite directions as the perturbation amplitude changes. This means that resonant perturbations produce simultaneously a stabilizing effect on one attractor, as was observed in experiments dealing with chaos suppression, and a destabilizing effect on the other attractor. We also demonstrate that bistability and shift of the bifurcation diagrams strongly depend on the phase difference between perturbation and fundamental frequencies.

Our investigations were performed on a CO_2 laser with modulated losses via an acousto-optic modulator inserted in the laser cavity. The experimental arrangement is similar to that described in previous works [2,6]. Two electric signals were applied to the modulator providing the time-dependent cavity losses. The driving signal, $V_1(t)\cos(2\pi ft)$, had the frequency $f=160$ kHz and the amplitude $V_1(t)$, which was periodically changed by a triangle law with a frequency 30 Hz. The perturbation signal, $V_2(\cos\pi ft+\varphi)$, had the frequency $f/2$, an amplitude V_2, and a phase φ. The relaxation-oscillation frequency f_r was about 100 kHz and thus, the ratio $m=f/f_r$ was approximately 1.6. The laser response was detected with a CdHgTe detector and the bifurcation diagrams were recorded by a Tektronix 2440 digital oscilloscope. We used the technique of stroboscopic data recording with a sampling period of $7T$ $(T=1/f)$.

In numerical simulations we used the following two-level rate-equation laser model [7]:

$$\frac{du}{dt}=\tau^{-1}(y-k)u, \quad \frac{dy}{dt}=(y_0-y)\gamma-uy, \tag{1}$$

where

$$k=k_0+k_1g(t)\cos(2\pi ft)+k_2\cos(\pi ft+\varphi), \tag{2}$$

$$g(t)=\sum_n g_n\cos[\pi(2n-1)Ft], \quad n=1,\ldots,12. \tag{3}$$

Here u is proportional to the radiation density, y and y_0 are the gain and the unsaturated gain in the active medium, respectively, τ is half round-trip time of light in a resonator, γ is the gain decay rate, k is the total cavity losses, k_0 is the constant part of the losses, k_1 is the driving amplitude, k_2 is the perturbation amplitude, φ is the perturbation phase, $g(t)$ describes the shape of the driving amplitude by a triangle law, where the coefficients g_n were calculated from the Fourier transform of the triangle shape, F is the frequency of a slowly varying triangle envelope of the driving amplitude. The following fixed parameters were used throughout our calculations: $\tau=3.5\times10^{-9}$ s, $\gamma=1.978\times10^5$ s^{-1}, $y_0=0.175$, $k_0=0{,}17\,303$, $F=30$ Hz, $m=1.6$. The parameters k_1, k_2, and φ were varied in our numerical simulations.

First, let us describe the results of the computer simulations. Figure 1 shows typical bifurcation diagrams of a modulated CO_2 laser obtained from rate equations (1) with triangle sweeping (3) of the driving amplitude, and stroboscopic sampling of the data. Figure 1(a) corresponds to for-

*On leave from B.I. Stepanov Institute of Physics, Academy of Sciences, Belarus, 220072 Minsk. Electronic address: lmk@dragon.bas-net.by
†Fax:+34-3-5812155. Electronic address: corbalanr@cc.uab.es

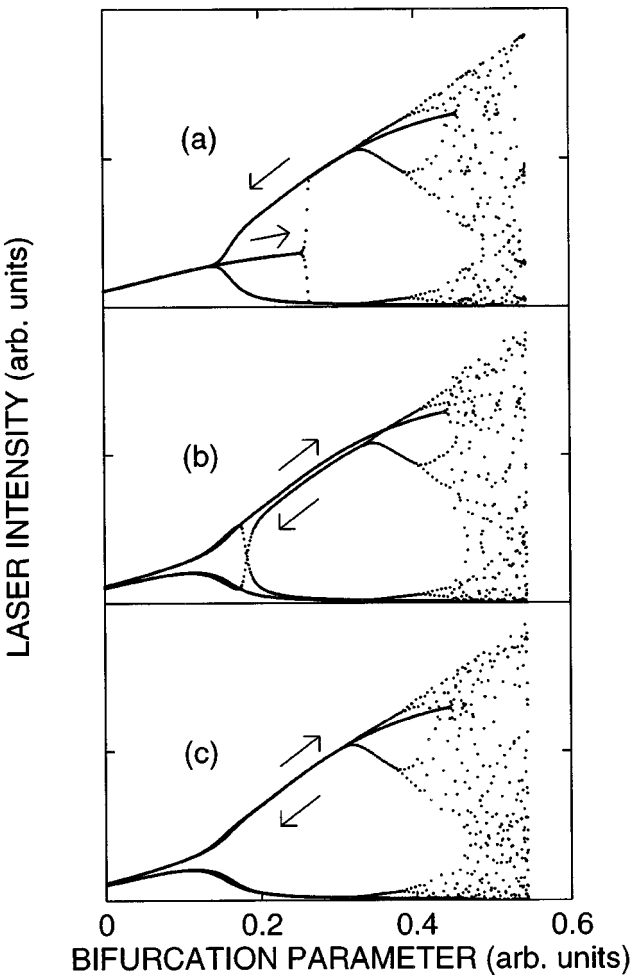

FIG. 1. Numerical bifurcation diagrams for a CO_2 laser vs the driving amplitude at forward and reverse sweeps: (a) without perturbation, (b) and (c) in the presence of the perturbation ($k_2=5.25\times10^{-5}$, $k_1=5.6\times10^{-3}$, $\varphi=0$).

ward and reverse sweeps of the driving amplitude without perturbation ($k_2=0$) and shows a dynamical distortion of the bifurcation diagram due to sweep effects, which have been studied earlier, both theoretically [8] and experimentally [9]. When a weak resonant perturbation of frequency $f/2$ is introduced, the primary solution splits into two solutions, which appear for the reverse sweep of the driving modulation. These two solutions are shown separately in Figs. 1(b) and 1(c), respectively. It is seen in Fig. 1(b) that the responses for forward and reverse sweeps do not coincide. The system comes back to the initial value of the driving amplitude ($k_1=0$) via a path which is different from the one in the forward sweep. Such a behavior is the one which appears most often in computer simulations. At the same time there exists the second solution shown in Fig. 1(c). In this case the laser responses for reverse and forward sweeps practically coincide for bifurcation parameters ranging from 0 to 0.35. At the latter value the $2T-4T$ bifurcation occurs and above it the dynamical distortion shows up. Because of this, we may consider these responses for forward and reverse sweeps in Fig. 1(c) as belonging to the same solution. In order to find this second solution in computer simulations we changed initial conditions. Figure 2 more clearly displays the splitting of the primary solution into two new solutions near

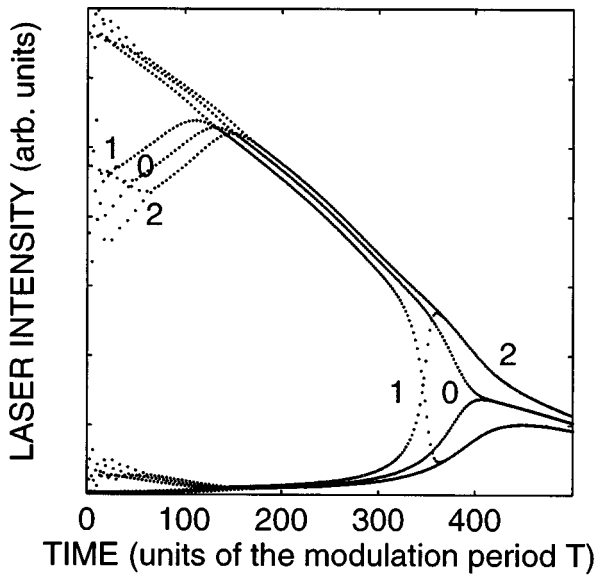

FIG. 2. A part of the bifurcation diagram at reverse sweep of the driving amplitude vs time (in units of the modulation period T) showing the splitting of a primary solution. Curve 0 is without perturbation, curves 1 and 2 are with a perturbation ($k_2=5.25\times10^{-5}$, $k_1=5.6\times10^{-3}$, $\varphi=0$).

the first three bifurcation points. When the driving amplitude reaches some critical value, which depends on the perturbation amplitude, solution-1 undergoes an inverse $2T-T$ bifurcation and becomes an unstable T periodical solution. After that the system rather quickly approaches the other coexisting stable solution (solution-2), by changing the phase in the response by π. This transition corresponds to a new location of the first bifurcation point shifted by the resonant perturbation. Thus, rather weak resonant perturbations induce bistability just above the first shifted period doubling bifurcation point and therefore drastically changes the nature of the system. At the upper-left hand side of Fig. 2, it is also seen that the resonant perturbation pushes the bifurcation points belonging to these new solutions in opposite directions.

Figure 3 shows the effect of periodic perturbations with different amplitudes and phases on both coexisting solutions. Only one period of the slow periodic shape of the driving amplitude is shown [Fig. 3(a)]. The system periodically alternates in time between two solutions. Such a periodic alternation in the laser response is obtained from direct computer simulations, and can therefore be considered as a natural temporal evolution of the system. In order to simplify Fig. 3, the part of solution-2 which coexists with solution-1 is not shown. As the perturbation amplitude increases [from Fig. 3(b) to Fig. 3(d)], all bifurcation points of solution-1 are shifted to a higher value of the driving amplitude and chaos in solution-1 disappears [Figs. 3(c) and 3(d)]. But at the same time all bifurcation points of solution-2 shift in an opposite direction towards lower values of the driving amplitude as the perturbation increases and one can see, in Fig. 3(d), the appearance of chaos. Thus, we can state that the resonant perturbation produces simultaneously stabilizing effects on one attractor and destabilizing effects on the other one. A further increase of the perturbation amplitude leads to a reduction of the parameter range of the driving amplitude where solution-1 exists. At some critical value of k_2 (this

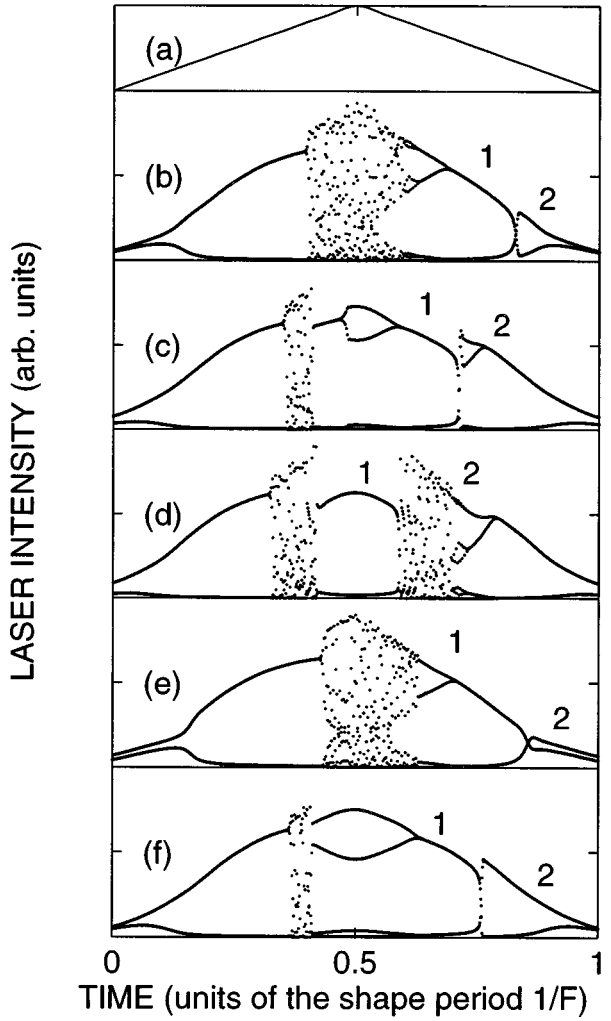

FIG. 3. Numerical bifurcation diagrams for a CO_2 laser vs time for different values of the perturbation amplitude k_2 and phase φ with a triangle shape of the driving amplitude shown in (a). $k_1=5.6\times10^{-3}$. (b), (c), and (d) $\varphi=0$, $k_2=7\times10^{-5}$, 3.5×10^{-4}, and 5.43×10^{-4}, respectively. (e) and (f) $k_2=2.1\times10^{-4}$, $\varphi=22°$ and 120°, respectively.

critical value essentially depends on the φ) the two attractors merge into a single one. For a given perturbation amplitude, the change in the phase from $\varphi\cong22°$ (where the minimal shift is observed) to $\varphi\cong120°$ strongly increases the shift of the bifurcation points [Fig. 3(e) and 3(f)]. For a quantitative characterization we show dependences of the shift of the first period doubling bifurcation point as a function of the phase φ (Fig. 4) and the perturbation amplitude k_2 [Fig. 5, at $\varphi=0$ (curve 1) and $\varphi=2\pi/3$ (curve 2), respectively]. The phase dependence of the shift is a π-periodical function and bears similarities to the phase dependence of a small signal amplification [10]. It should be noted that dependence of the shift on the perturbation amplitude cannot be characterized by a simple scaling law throughout the entire range of change of the perturbation amplitude. However, it is possible to distinguish two regions of the perturbation amplitude where some scaling properties may be derived from the numerical data. In the first region for the perturbation amplitude going from 6.25×10^{-3} to 3.75×10^{-2} (here k_2 normalized to the value of the driving amplitude k_1), the shift is approximately proportional to k_2^{α}, where α is a π-periodical function of the

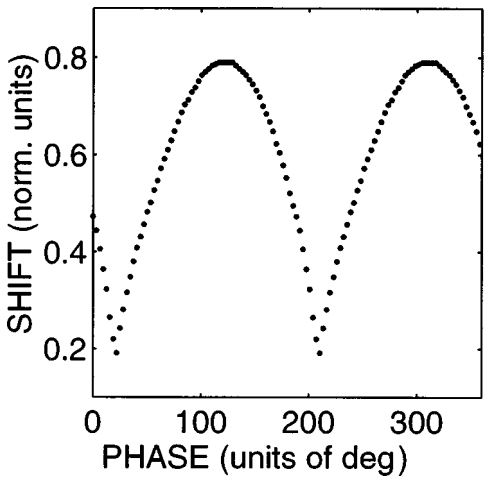

FIG. 4. The phase dependence of the shift of the first period doubling bifurcation point obtained numerically (normalized to the threshold of period doubling with zero applied perturbation). $k_1=5.6\times10^{-3}$, $k_2=2.1\times10^{-4}$.

perturbation phase φ (e.g., $\alpha=0.82$ at $\varphi=0°$ and $\alpha=0.71$ at $\varphi=120°$, $F=30$ Hz) and also depends on the frequency F. In the second region for the perturbation amplitude going from 5×10^{-2} to 0.125×10^{-2} the shift is approximately proportional to $\exp(\beta k_2)$, where β is also a π-periodical function (e.g., $\beta\cong18.7$ at $\varphi=0°$ and $\beta\cong20.8$ at $\varphi=120°$, $F=30$ Hz), but contrary to the first region, it almost does not depend on the sweeping frequency F. Really, these scaling properties cannot be considered as exact scaling laws for the shift because the power in scaling laws depends on the range of the perturbation amplitude where they are derived. However, the scaling properties found may be valid for other nonautonomous systems if operating in the same ranges of normalized perturbation amplitude. The scaling laws may be derived more exactly in the limit $F\to0$.

It is worth noting that the presence of the resonant perturbation changes the power in the scaling law which relates the

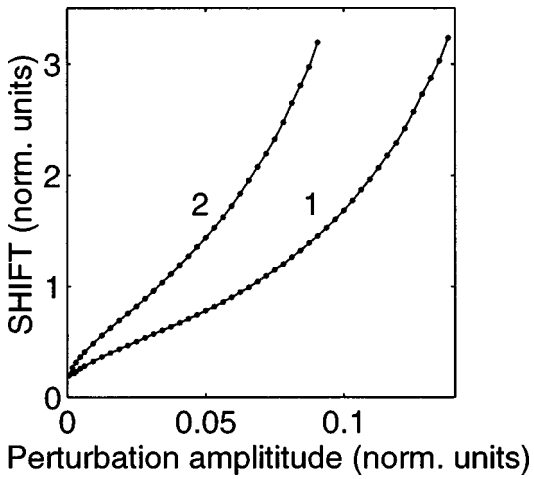

FIG. 5. Shift of the first period doubling bifurcation point as a function of the perturbation amplitude k_2 for different values of the phase φ obtained numerically. Shift is normalized to the threshold of period doubling with zero applied perturbation. $k_1=5.6\times10^{-3}$, k_2 is normalized to the value of the driving amplitude k_1; curve 1 — $\varphi=0°$, curve 2 — $\varphi=120°$.

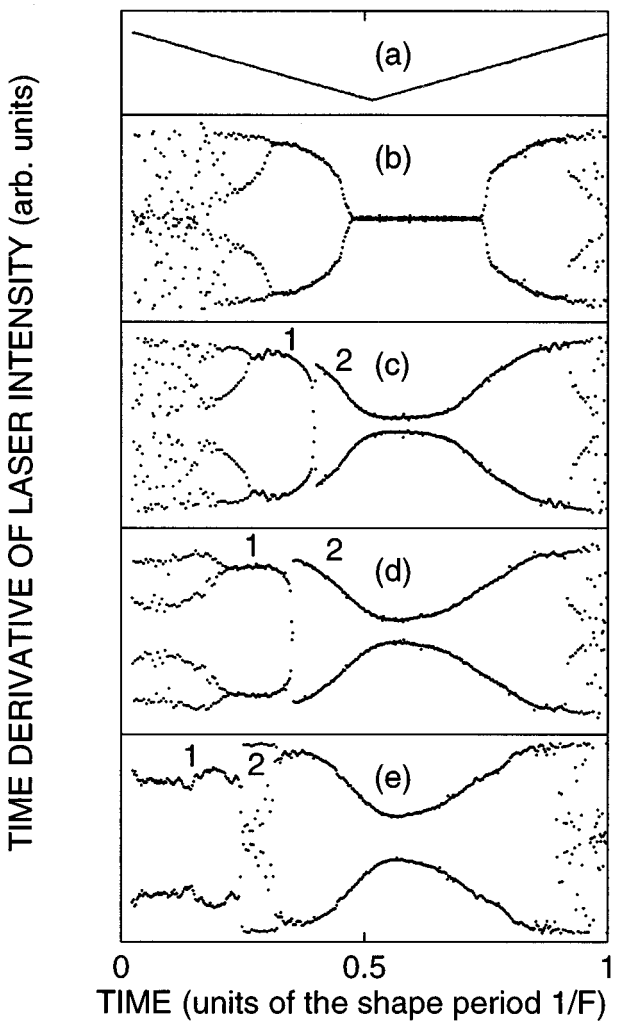

FIG. 6. The time derivative of the experimental bifurcation diagrams of a CO_2 laser vs time for different values of the perturbation amplitude V_2 at the frequency $f/2$ with a triangle shape of the driving amplitude V_1 (a). (b) $V_2=0$ (without perturbation), (c) $V_2=2.5V$, (d) $V_2=5V$, and (e) $V_2=9V$. Here $\varphi=0$.

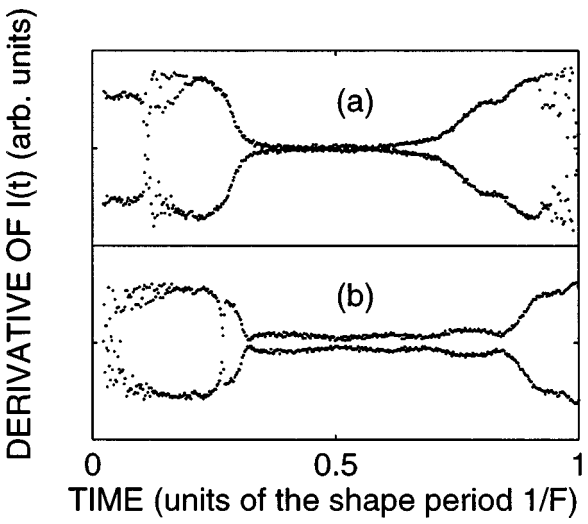

FIG. 7. The time derivative of experimental bifurcation diagrams of a CO_2 laser vs time for two values of the perturbation phase φ which differ approximately by $\pi/3$ ($V_2=4$ V).

delay of the first bifurcation to the frequency of the slowly varying shape (or sweep rate) of the driving amplitude. Kapral and Mandel have predicted for the nonautonomous quadratic map that this delay is proportional to the square root of the sweep rate of the control parameter [8]. In our computer simulations we explored a range of frequencies F from 1 Hz – 40 Hz, and we found that without perturbation the delay δ is proportional to F^{η}, where $\eta=0.51$, that practically coincides with this theoretical prediction. With the resonant perturbations at frequency $f/2$ the delay δ is also proportional to F^{η}, but in this case η is a π-periodical function of the perturbation phase φ and slightly also depends on the perturbation amplitude k_2. For example, for $\varphi=0$ the value of η is equal $\simeq 0.64$ in the range of perturbation amplitudes going from 6.25×10^{-3} to 6.25×10^{-2}, and $\eta \simeq 0.667$ for $k_2=0.125$.

Although we are not seeking here for a quantitative agreement between theory and experiment, the experimental investigations qualitatively confirm all the main conclusions obtained from numerical simulations. Figure 6 shows experimental bifurcation diagrams versus time (in units of the shape period $1/F$) for different values of the amplitude of the resonant perturbation at the frequency $f/2$. In order to more clearly reveal the location of all bifurcation points we represent the time derivative of the bifurcation diagrams. In the absence of the perturbation, the diagram in Fig. 6(b) shows delayed bifurcations at a forward sweep with respect to a reverse sweep. When we introduce the perturbation, one clearly sees (i) the appearance of two branches [which for the reverse sweep look very similar to the solutions obtained numerically (compare Fig. 3 and Fig. 6)] and, correspondingly, the appearance of bistability, (ii) the transition between two coexisting branches with a π phase shift in the laser response, that corresponds to reaching the unstable T orbit in the first branch, and (iii) opposite shifts of all bifurcation points belonging to these two different coexisting attractors, so that the first attractor is stabilized while the second one is destabilized as the perturbation amplitude increases [Figs. 6(c)–6(e)]. We also found experimentally that the shift strongly depends on the perturbation phase (Fig. 7) and amplitude (Fig. 8). For the given perturbation amplitude the maximal shift was observed at $\varphi\cong120°$, and the minimal shift was observed at $\varphi\cong25°$, these are in a good agreement with theoretical predictions. We also checked experimentally that dependence of the shift on the phase φ is a π-periodical function. In our experiments we did not know exactly the amplitude of the losses perturbation (k_2) and, as a consequence, we could not make a direct comparison of the experimental shift as a function of the applied perturbation voltage (V_2) with the numerical results. But similar to the numerical results, we distinguish two regions where experimental shift may be characterized by some scaling properties. In the first region of applied perturbation voltage V_2 going from 0.1 V–4.5 V, the experimental shift is approximately proportional to V_2^{α} with $\alpha\cong0.71$, and in the second region of V_2 from 5 V–9.9 V the shift is approximately proportional to $\exp(\beta V_2)$ with $\beta\cong14.5$. Both values are rather close to the numerical results.

In order to prove the appearance of bistability, not only in the dynamical regime so far discussed, we performed well-

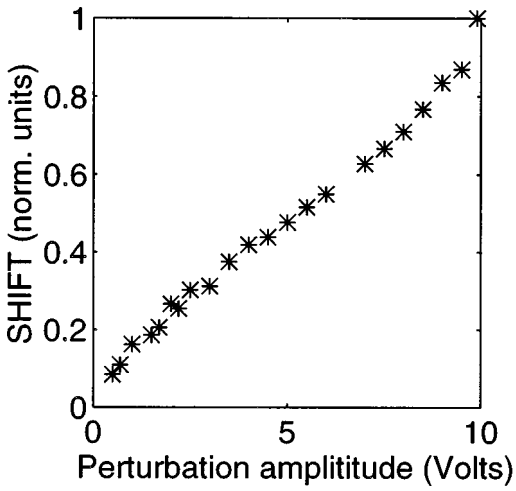

FIG. 8. Experimental shift of the first period doubling bifurcation point as a function of the perturbation amplitude V_2 for $\varphi=0$.

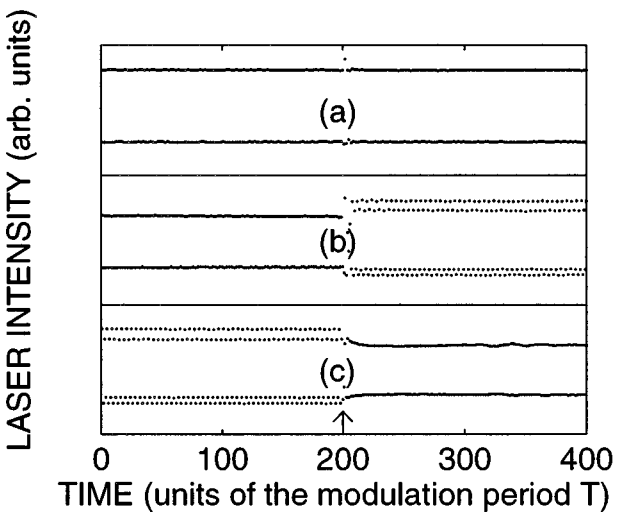

FIG. 9. Experimental switchings between coexisting attractors in the bistability domain induced by the resonant perturbation at the frequency $f/2$. (a) Initial state (without perturbation at $f/2$), (b) forward switching, and (c) reverse switching.

controlled switchings in the bistability domain induced by the resonant perturbation also in the case of a constant driving amplitude. For this purpose the technique of short-lived losses perturbation was used [11]. Acting by single short-lived loss perturbation we may switch from one attractor to the other one and vice versa. The effect of a short-lived loss perturbation is equivalent to a change in initial conditions. This means that the system can be sent, instantaneously as compared to characteristic times of the system, from the first attractor to the basin of attraction of the second attractor, so that the latter may appear in the response. In Fig. 9(a) we show the initial $2T$ orbit without resonant perturbation at frequency $f/2$ with a short transient after the action (the arrow in Fig. 9) of a short-lived losses perturbation. For these experimental conditions we found only one attractor. After turning on the resonant perturbation at the frequency $f/2$, bistability appears in the system. Figures 9(b) and 9(c) show forward and reverse switchings between the two coexisting attractors which appeared instead of the primary attractor. Similar switchings were observed for wide ranges of values of the bifurcation parameter, and of the amplitudes and phases of resonant perturbations.

To conclude, we have shown that weak resonant perturbations fundamentally modify the nature (phase space) of nonautonomous systems by splitting a primary attractor into two new ones. We have also demonstrated that they simultaneously produce a stabilizing effect on one attractor and a destabilizing effect on the other one. It is particularly remarkable that by introducing weak parametric perturbation, one obtains a completely different system, with the possibility to control at will the overlapping of dynamical regimes associated with new coexisting attractors, by changing the amplitude and the phase of resonant perturbations, as well as the bifurcation parameter. Switchings between these two coexisting attractors can be easily produced using the technique of short-lived large-amplitude perturbations as shown here.

V.N.C. is indebted to the DGICYT (Spain) for a grant (Grant No. SB94-A26). A.N.P. acknowledges support from the Generalitat de Catalunya. Financial support from the DGICYT (Project No. PB95-0778-C02-02) is also acknowledged.

[1] R. Lima and M. Petttini, Phys. Rev. A **41**, 726 (1990); Y. Braiman and I. Goldhirsch, Phys. Rev. Lett. **66**, 2545 (1991); L. Fronzoni, M. Giocondo, and M. Pettini, Phys. Rev. A **43**, 6483 (1991); M. Salerno, Phys. Rev. B **44**, 2720 (1991); R. Chacon and J. D. Bejarano, Phys. Rev. Lett. **71**, 3103 (1993); W. X. Ding, H. Q. She, W. Huang, and C. X. Yu, *ibid.* **72**, 96 (1994); R. Meucci, W. Gadomski, M. Ciofini, and F. T. Arecchi, Phys. Rev. E **49**, R2528 (1994); Z. Qu, G. Hu, G. Yang, and G. Qin, Phys. Rev. Lett. **74**, 1736 (1995); R. Metlin, A. Hubler, A. Scheeline, and W. Lauterborn, Phys. Rev. E **51**, 4065 (1995); P. Colet and Y. Braiman, *ibid.* **53**, 200 (1996).

[2] V. N. Chizhevsky and R. Corbalán, Phys. Rev. E **54**, 4576 (1996).

[3] It should be noted that near-resonant perturbations can also induce or suppress chaos [S. T. Vohra, L. Fabiny, and F. Bucholtz, Phys. Rev. Lett. **75**, 65 (1995)].

[4] A. Gavrilides, P. M. Alsing, V. Kovanis, and T. Erneux, Opt. Commun. **115**, 551 (1995).

[5] E. Ott, C. Grebogi, and J. A. Yorke, Phys. Rev. Lett. **64**, 1196 (1990).

[6] R. Corbalán, J. Cortit, A. N. Pisarchik, V. N. Chizhevsky, and R. Vilaseca, Phys. Rev. A **51**, 663 (1995).

[7] J. R. Tredicce, F. T. Arecchi, G. P. Puccioni, A. Poggi, and W. Gadomski, Phys. Rev. A **34**, 2073 (1986).

[8] R. Kapral and P. Mandel, Phys. Rev. A **32**, 1076 (1985).

[9] D. Dangoisse, P. Glorieux, and D. Hennequin, Phys. Rev. A **36**, 4775 (1987).

[10] P. Glorieux, C. Lepers, R. Corbalán, J. Cortit, and A. N. Pisarchik, Opt. Commun. **118**, 309 (1995).

[11] V. N. Chizhevsky and S. I. Turovets, Opt. Commun. **102**, 175 (1993); Phys. Rev. A **50**, 1840 (1994); V. N. Chizhevsky and P. Glorieux, Phys. Rev. E **51**, R2701 (1995).